Real-Time Control Plane Operations for gOSNR QoT Estimation through OSNR Monitoring

Alan A. Díaz-Montiel[†], Ayush Bhardwaj[†], Bob Lantz[*], Jiakai Yu[*], Aamir N. Quraishy[*], Dan Kilper[†*] and Marco Ruffini[†]

[†]*CONNECT Centre, Trinity College Dublin, Ireland,* [*] *University of Arizona, USA.*
alan.diaz@connectcentre.ie

Abstract: We analyze an optical control plane algorithm designed to operate in real-time to improve generalized-optical signal-to-noise ratio (gOSNR) quality-of-transmission-estimation (QoT-E), based on OSNR monitoring. We report QoT-E performance improvements of up to 1 dB.

1. Introduction

Optical network disaggregation has recently emerged as a networking model to enable the use of multi-vendor components in optical systems. This has also advanced the development of open software-defined networking (SDN) control planes. However, the use of heterogeneous components can increase uncertainty on system performance, for example reducing the predictability of quality of transmission (QoT). This in turn imposes the use of large optical signal-to-noise ratio (OSNR) margins, which adversely affects network efficiency and complicates fault diagnosis. For this reason, improving QoT estimation (QoT-E) and monitoring has become a key target for open systems. Although analytical systems have been used for estimation of fibre nonlinearities [1], the use of active components, such as erbium-doped fiber amplifiers (EDFAs) create uncertainty that is difficult to model analytically. This is again exacerbated by the component vendor diversity in disaggregated optical systems.

In order to improve lightpath QoT-E, the use of machine-learning (ML) algorithms has received much attention [2,3]. While promising, the practical application of ML estimation models in operational networks is complicated by the need for large data sets, including in-service performance measures. An alternative technique is the use of components for real-time monitoring of OSNR in selected network locations, which can provide data and/or reduce the need for large data sets. Meng *et al.* [5] have proposed a real-time OSNR monitoring algorithm that can intelligently select which optical signals to monitor in an optical link, and use this information to infer the OSNR levels of neighboring signals. Another option is the use of coherent receivers to estimate lightpath QoT given the characteristics of the optical link, which can effectively provide gOSNR monitoring as well as other power anomaly detection measures through digital backpropagation [4,6].

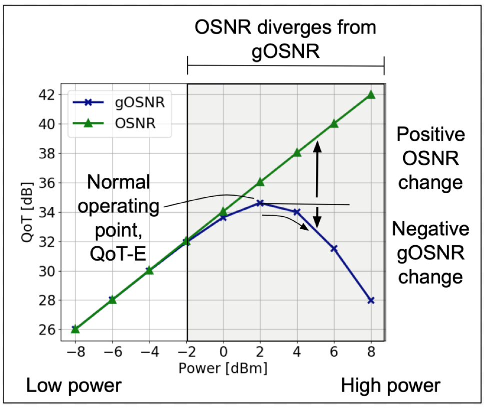

Fig. 1: Difference between OSNR and gOSNR for increasing power levels, leading to QoT-E inaccuracy.

In this paper, we address two key questions for the control and prediction of QoT in disaggregated optical systems, which can be used both for fault management as well as lightpath QoT-E for dynamic wavelength routing. Firstly, we analyze the error that OSNR vs generalized-OSNR (gOSNR) monitoring produce in estimating QoT for different numbers of optical performance monitors (OPMs) deployed in an optical link. Secondly, we show how real-time OSNR monitoring information can be used to improve the QoT-E and monitoring functions, even when only OSNR types of OPM are available. For this, we introduce an OSNR monitoring-based channel modeling solution. It should be noted that we do not focus on specific device performance, instead we study monitoring strategies at the network scale and how they can be used effectively to monitor and estimate QoT across the network given uncertainties inherent in the systems.

In particular, we address the complication of OSNR monitoring considering that the OSNR is inversely related to the gOSNR for high transmission power, as shown in Figure 1. Thus, for a channel whose power is higher than originally estimated, OSNR monitoring alone would indicate that the QoT is higher than the QoT-E. However, since the nonlinear interference increases with absolute power, at high transmission power (e.g. due to gain ripple power divergence), the presence of nonlinear interference renders the actual QoT lower than its OSNR-based value would indicate. This is particularly important for monitoring scenarios in which the noise figure of an amplifier can be expected to be relatively constant, but the channel powers will vary based on the loading scenario, which is the main focus of this work.

In this work we use an optical control plane application capable of retrieving live OSNR information from OPMs in the network and use it to determine the QoT to compare that with the QoT-E based on design parameters alone, without any monitoring. Our control plane operations were tested with the Mininet-Optical [7] packet-optical network emulator, which allows testing of optical control planes over large size virtual optical network topologies.

2. Optical SDN control plane algorithms

First introduced in [7], Mininet-Optical enables the development and testing of optical SDN control plane algorithms by providing a south-bound interface to emulated optical components (i.e., transponders, ROADMs, EDFAs and OPMs). Thus, researchers can test their control plane algorithms and operations in a virtual environment, which reproduces both control elements and physical impairments of a real disaggregated optical network. Mininet-Optical models the physical effects of optical network transmission (i.e., optical signal power propagation, Stimulated Raman Scattering (SRS), single- and cross-channel interference (SCI and XCI)). The latter is used to model the gOSNR, and it is based on the nonlinear noise model found in the GNPy project [8]. Additionally, it simulates the wavelength-dependent gain of EDFAs, which is one of the main sources of uncertainty in QoT-E models, providing a more realistic environment to test the performance of QoT-E algorithms. The monitoring capabilities of Mininet-Optical allow us to collect optical signal power, ASE and NLI noise data of individual channels and study collective effects that can manifest over a large network. The collection of this data is enabled through virtual OPM components that emulate OSNR monitors or reference receivers [4] that can recover estimates of the full gOSNR, either of which can be interrogated through a control plane interface. We can place these OPM modules at any location of an optical link. Thus, the data collected from these monitors can be used in ML algorithms to better diagnose faults or control the network.

In order to provide a comparison for our control plane QoT-E implementation, we produce a baseline estimation algorithm that is typical of offline planning tools (e.g., GNPy integration with the ONOS controller [8]). This baseline estimation is provided considering, for any given optical transmission, the ASE and NLI noise levels for every channel at every location that the channels traverse.

OSNR/gOSNR estimation and correction algorithm

In this study, we look at how OPM monitoring at intermediate nodes in a link can help to improve the estimation of gOSNR levels of individual channels along a path. We use the estimated power (P_E), ASE noise (ASE_E) and NLI noise (NLI_E) to compute the estimated gOSNR with $gOSNR_E = P_E/(ASE_E + NLI_E)$. We test three different types of gOSNR estimation models: **model (i)** updates the ASE noise levels from the baseline model estimate based on the expected noise levels given by the OSNR monitoring, where it is available; **model (ii)** uses this OSNR monitoring information together with channel monitoring information to build a model for the optical power levels between monitoring points and gOSNR estimates based on these values; **model (iii)** uses reference receiver monitors that directly measure gOSNR, which is used to set the QoT values to perform subsequent estimations along the path.

More specifically, in model (i) we replace the P_E and ASE_E values in the QoT-E procedure by the monitored power P_M and ASE noise ASE_M. These updated performance metrics are then used to compute the QoT-E at the subsequent locations in the optical link. Note that such OSNR monitoring is sensitive to uncertainties in the amplifier noise figures, which would be reflected in the ASE noise power measurement. We then propose model (ii), where in addition to the operations in model (i), we also compute the difference between P_E and P_M to produce a NLI_E correction factor, p_{corr}, for the gOSNR estimation formula. This measured power difference is then assumed to be uniformly distributed among each span between monitoring locations (i.e. assuming a linear ramp). Thus, at every OPM location i, for every channel ch, we compute $p\_corr_{ch_i} = |Pm_{ch_i}/Pe_{ch_i}|^3$ for the nonlinear noise and ramping it for each span between monitoring locations. Then we apply this correction factor to NLI_E, resulting in a corrected NLI noise (NLI_C), which is used to compute an updated $gOSNR_E$. Last, model (iii) replaces all estimated metrics by direct gOSNR measurements, effectively resetting the QoT-E to a new starting value at that node for use in subsequent estimation along the path. Model (iii) provides the most accurate results and requires more expensive reference receivers. It is important to understand the relative merits of different monitoring strategies to balance against their potential costs.

3. System setup and results

With Mininet-Optical we model the Cost239 European Network topology with 11 nodes and 26 links. For this analysis, we focus on the London to Copenhagen link, measuring 1000 km, composed of 20x50km fibre spans. We assume that all spans are optically compensated by EDFAs with target gains of 11 dB. Then, our optical SDN controller configures the transponders to set the wavelength channels and launch power. Also, the controller must configure the ROADM nodes to switch lightpaths appropriately. We include a boost amplifier after every ROADM, compensating for an overall insertion loss of 17 dB. We also include channel power equalization procedures at the ROADM nodes and at every 6th span in the links, carried out through variable optical attenuators (VOAs) in the ROADMs or equivalent channel gain equalizers.

Our first goal is to analyze the performance of the three models presented in Section 2 to assist gOSNR estimation. Thus, we configured a 15-channel transmission configuration to traverse the link. The 15-channel set was randomly allocated in the C-band channels (191.6 - 195.6 THz), with channel spacing of 50GHz and launch power of 0 dBm per channel. In Figure 2a we show the performance of the three models when OPMs are co-located with channel leveling locations (every 6th span), in addition to each intermediate location between these. Thus, we consider 8 OPM nodes out of 21 possible locations (evenly-spaced across the link). In the figure, the green solid curve represents the maximum error produced by the baseline QoT-E model (when we do not monitor at any location). This maximum QoT error is computed considering the estimations for all 15 channels, predicted at each potential monitoring location. The light-blue curves correspond to the performance of model (i) described above, the red curves to model (ii), and the dark-blue curves to model (iii). We can see that simply correcting data points with OSNR information (model (i)) reduces the error compared to the unmonitored scenario. However, peak errors are still similar. Here we consider peak errors as the main indicator of estimator performance, as these will affect most the required system margins. The key finding is that our proposed model (ii) (red curve) is able to lower the peak error by over 0.5 dB, using the exact same amount of OSNR information. Indeed it is capable of reducing peak errors considerably.

Figure 2b focuses on the trade-off between the model used and the number of OPM locations. Here we can see that even with a higher number of OPM locations (16 out of 21 locations), simply correcting OSNR data points (model (i)) is not effective in reducing the peak estimation error, which remains similar to the unmonitored curve at location 11. Our proposed model (ii) can instead reduce the peak error by 0.7 dB, even using a smaller number of OPMs (12 are considered here). Comparing the red and dark blue curve, we can also notice the we can trade simple OSNR monitors with more complex gOSNR solutions, if we increase their number. When coupled with our proposed model (ii), using 12 ONSR monitors provides comparable peak error (0.1 dB lower) than using 6 gOSNR monitors.

The comparison between the three models as a function of the number of OPM locations, is finally reported in Figure 2c, which reports the peak error for each scenario. We can observe that model (ii) outperforms model (i) by up to 1 dB. In addition, for increasing number of OPM locations, the discrepancy with model (iii) is reduced to less than 0.5 dB.

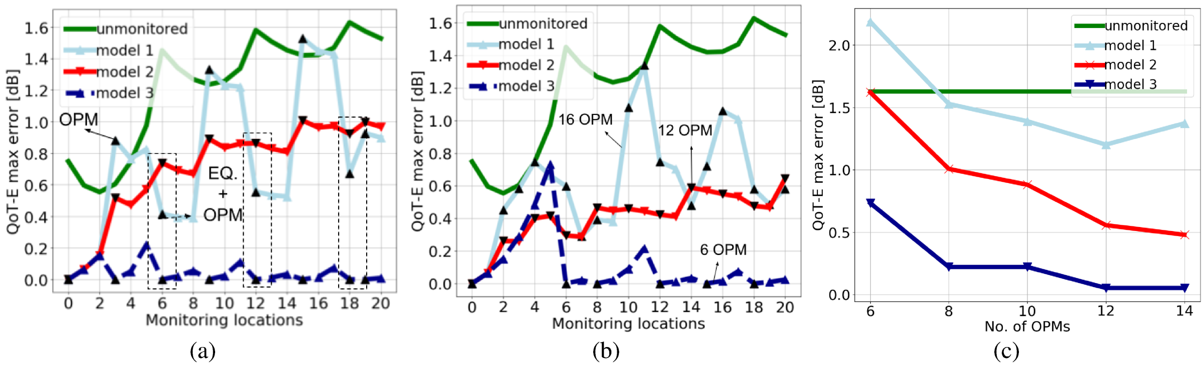

Fig. 2: *(a)*: comparison of different QoT-E correction models with 8 OPMs; *(b)*: comparison of model (i) with 16 OPMs, model (ii) with 12 and model (iii) with 6; *(c)*: comparison of the impact of increasing the number of OPM locations for the three models.

Acknowledgments

Financial support SFI grants 18/RI/5721, 14/IA/2527 and NSF grant 2029295 is gratefully acknowledged.

References

1. R. Wang, et al., Load-aware nonlinearity estimation for elastic optical network resource optimization and management. JOCN, May'19.
2. A. D'Amico et al., Using machine learning in an open optical line system controller. JOCN June'20.
3. F. Locatelli, et al. Machine Learning-based in-band OSNR Estimation from Optical Spectra. PTL, Oct.'19.
4. M. Bouda et al., Accurate prediction of quality of transmission based on a dynamically configurable optical impairment model. JOCN, Jan'18
5. F. Meng, et al. Self-Learning Monitoring on-demand Strategy for Optical Networks. JOCN, Mar.'19.
6. T. Tanimura, et al. Fiber-Longitudinal Anomaly Position Identification over Multi-Span Transmission Link out of Receiver-End Signals. JLT, Apr.'20.
7. B. Lantz, et al. Demonstration of Software-Defined Packet-Optical Network Emulation with Mininet-Optical and ONOS. M3Z.9, OFC'20.
8. J. Kundrát, et al. Physical-Layer Awareness: GNPy and ONOS for End-to-End Circuits in Disaggregated Networks. M3Z.17, OFC'20.